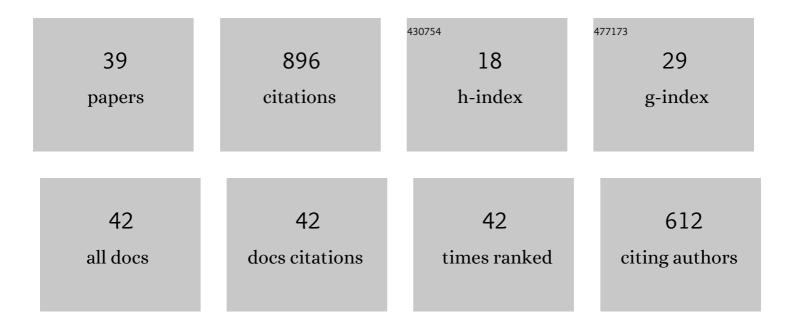
Hongchao Kou

List of Publications by Year in descending order

Source: https://exaly.com/author-pdf/9556207/publications.pdf Version: 2024-02-01



#	Article	IF	CITATIONS
1	β to ω transformation strain associated with the precipitation of α phase in a metastable β titanium alloy. Journal of Materials Science, 2021, 56, 1685-1693.	1.7	15
2	The ω phase transformation during the low temperature aging and low rate heating process of metastable β titanium alloys. Materials Chemistry and Physics, 2020, 239, 122125.	2.0	16
3	Texture evolution and the recrystallization behavior in a near Î ² titanium alloy Ti-7333 during the hot-rolling process. Materials Characterization, 2020, 159, 109999.	1.9	27
4	A brief review of data-driven ICME for intelligently discovering advanced structural metal materials: Insight into atomic and electronic building blocks. Journal of Materials Research, 2020, 35, 872-889.	1.2	17
5	Ϊ‰-Assisted refinement of α phase and its effect on the tensile properties of a near β titanium alloy. Journal of Materials Science and Technology, 2020, 44, 24-30.	5.6	33
6	When a defect is a pathway to improve stability: a case study of the L12 Co3TM superlattice intrinsic stacking fault. Journal of Materials Science, 2019, 54, 13609-13618.	1.7	16
7	Interstitial triggered grain boundary embrittlement of Al–X (X =†H, N and O). Computational Materials Science, 2019, 163, 241-247.	1.4	8
8	Dependence of mechanical properties on the microstructure characteristics of a near β titanium alloy Ti-7333. Journal of Materials Science and Technology, 2019, 35, 48-54.	5.6	41
9	Insight into solid-solution strengthened bulk and stacking faults properties in Ti alloys: a comprehensive first-principles study. Journal of Materials Science, 2018, 53, 7493-7505.	1.7	17
10	Precipitation behavior of Î \pm phase during aging treatment in a Î ² -quenched Ti-7333. Materials Characterization, 2018, 140, 275-280.	1.9	25
11	Kinetic Diffusion Couple for Mapping Microstructural and Mechanical Data on Ti–Al–Mo Titanium Alloys. Materials, 2018, 11, 1112.	1.3	6
12	In situ Observation of the Initial Stage of <i>γ</i> Lamella Formation in Ti48Al2Cr2Nb Alloy. Advanced Engineering Materials, 2017, 19, 1600670.	1.6	2
13	Composite structure of α phase in metastable β Ti alloys induced by lattice strain during β to α phase transformation. Acta Materialia, 2017, 132, 307-326.	3.8	80
14	The origin of striation in the metastable β phase of titanium alloys observed by transmission electron microscopy. Journal of Applied Crystallography, 2017, 50, 795-804.	1.9	20
15	Characteristics of a hot-rolled near \hat{l}^2 titanium alloy Ti-7333. Materials Characterization, 2017, 129, 135-142.	1.9	35
16	Microstructure and hydrogen storage properties of Mg-Ni-Ce alloys with a long-period stacking ordered phase. Journal of Power Sources, 2017, 338, 91-102.	4.0	62
17	Precipitation of α phase and its morphological evolution during continuous heating in a near β titanium alloy Ti-7333. Materials Characterization, 2017, 132, 199-204.	1.9	32
18	Phase precipitation behavior during isothermal deformation in β-quenched near beta titanium alloy Ti-7333. Journal of Alloys and Compounds, 2016, 671, 381-388.	2.8	31

Нолсснао Кои

#	Article	IF	CITATIONS
19	Microstructure and mechanical property correlation and property optimization of a near Î ² titanium alloy Ti-7333. Journal of Alloys and Compounds, 2016, 682, 517-524.	2.8	66
20	Non-isothermal synergetic catalytic effect of TiF3 and Nb2O5 on dehydrogenation high-energy ball milled MgH2. Materials Chemistry and Physics, 2016, 183, 65-75.	2.0	21
21	Microstructure and electrochemical hydrogenation/dehydrogenation performance of melt-spun La-doped Mg2Ni alloys. Materials Characterization, 2015, 106, 163-174.	1.9	29
22	Interdiffusion in FCC Co-Al-Ti Ternary Alloys. Journal of Phase Equilibria and Diffusion, 2015, 36, 127-135.	0.5	10
23	Microstructure Characterization and Mechanical Properties of In Situ Synthesized Ti ₂ <scp>A</scp> I <scp>N</scp> Ti48 <scp>A</scp> I2 <scp>C</scp> r2 <scp>N</scp> b Composites. Advanced Engineering Materials, 2014, 16, 507-510.	1.6	17
24	Hydrogen desorption performance of high-energy ball milled Mg 2 NiH 4 catalyzed by multi-walled carbon nanotubes coupling with TiF 3. International Journal of Hydrogen Energy, 2014, 39, 19672-19681.	3.8	51
25	Diffusion Research in BCC Ti-Al-Mo Ternary Alloys. Metallurgical and Materials Transactions A: Physical Metallurgy and Materials Science, 2014, 45, 1647-1652.	1.1	44
26	Precipitation of nanosized DO22 superlattice with high thermal stability in an Ni–Cr–W superalloy. Scripta Materialia, 2014, 76, 49-52.	2.6	18
27	Effect of strain rate on impact response and ï‰ transformation of quenched Zr–Nb alloys. Materials Characterization, 2013, 84, 10-15.	1.9	5
28	Hydrogenation behavior of high-energy ball milled amorphous Mg2Ni catalyzed by multi-walled carbon nanotubes. International Journal of Hydrogen Energy, 2013, 38, 16168-16176.	3.8	21
29	Evolution of the secondary $\hat{I}\pm$ phase morphologies during isothermal heat treatment in Ti-7333 alloy. Journal of Alloys and Compounds, 2013, 577, 516-522.	2.8	53
30	On the amorphization behavior and hydrogenation performance of high-energy ball-milled Mg2Ni alloys. Materials Characterization, 2013, 80, 21-27.	1.9	24
31	A phase-field approach to athermal $\hat{l}^2 \hat{a}^{\dagger} \hat{l}^{\infty}$ transformation. Computational Materials Science, 2012, 53, 187-193.	1.4	21
32	Modeling of Incommensurate ω Structure in the Zr-Nb Alloys. Metallurgical and Materials Transactions A: Physical Metallurgy and Materials Science, 2012, 43, 2581-2586.	1.1	2
33	Macrosegregation Behavior of Ti-10V-2Fe-3Al Alloy During Vacuum Consumable Arc Remelting Process. Journal of Materials Engineering and Performance, 2011, 20, 65-70.	1.2	6
34	Finite element simulation on the deep drawing of titanium thin-walled surface part. Rare Metals, 2010, 29, 108-113.	3.6	6
35	Microstructure Changes in Zr-Based Metallic Class Induced by Ion Milling. Rare Metal Materials and Engineering, 2010, 39, 1693-1696.	0.8	4
36	Deposition of Fe-based metallic glass coatings by Air Plasma Spraying process. International Journal of Surface Science and Engineering, 2010, 4, 288.	0.4	1

3

#	Article	IF	CITATIONS
37	Microstructure, phase and microhardness distribution of laser-deposited Ni-based amorphous coating. International Journal of Surface Science and Engineering, 2010, 4, 296.	0.4	10
38	Fabrication and Microstructure Characteristic of YBCO Bulk by Directional Top-Seeded Power Melting Process. Rare Metal Materials and Engineering, 2008, 37, 1893-1897.	0.8	0
39	Effects of Ta addition on the microstructure and mechanical properties of Ti40Zr25Ni8Cu9Be18 amorphous alloy. International Journal of Minerals, Metallurgy, and Materials, 2007, 14, 31-35.	0.2	3